Effect of Moisture on Thermal Performance and Energy Efficiency of Buildings with Lightweight Concrete Walls

Dariusz Gawin, Technical University of Lodz (Poland)
Jan Kosny, André Desjarlais, Oak Ridge National Laboratory

ABSTRACT

The main objective of this paper is to analyze the moisture effect on the steady-state and dynamic thermal performance of residential and commercial buildings located in California when Lightweight Concrete (LC) is applied as a material for wall construction. The thermal conductivity of five types of LC at various moisture contents was measured. Then, the annual record of moisture distribution in a LC wall was generated for California climatic conditions using HMTRA, a sophisticated computer model of coupled heat and moisture transfer in building materials. Based on the simulation results, the monthly average moisture content was calculated for evaluation of effective thermal properties of the LC wall during successive months after building construction. These data were applied to calculate the energy use during the first three years of building service time. A ranch style residential house and a commercial building located in Sacramento, California were analyzed using the DOE 2.1E computer model. For comparison, the annual energy consumption of similar buildings, with the same thermal resistance of the walls but constructed using steel studs and wood frame walls, was calculated. The LC wall house was the most energy efficient, for both residential and commercial buildings.

Introduction

Lightweight concrete as building material has been widely used in Europe for many years, but it is still not very popular in the U.S.A. One of the main problems associated with its application for house construction is the considerable decrease of thermal resistance with higher moisture content. The thermal conductivities of three different types of Autoclaved Aerated Concrete (AAC) blocks with densities of 400, 500 and 600 kg/m^3, wood concrete (Kosny 1994) and concrete with the foam beads aggregate (EPS concrete), for various hygroscopic moisture contents, were measured in ORNL's Material Properties Laboratory using the ASTM C-518 procedure. This is a steady-state method, which is usually used for dry materials. However it is much more accurate than unsteady-state methods, which are usually based on an analytical solution for an impulse-type change of boundary conditions, which is very difficult to obtain during tests. A detailed numerical analysis of heat and moisture transfer, taking into account phase changes during the steady-state measurements, was done in order to improve the accuracy of the steady-state measurements for moist lightweight concrete. For this purpose HMTRA, a computer code for the analysis of hygro-thermal behavior of porous building materials, was used. Approximate formulae expressing the thermal conductivity of the moist material, measured by use of an improved steady-state method as a function of moisture content, were found for the analyzed materials by use of the Least Squares Method.

The same computer code was used for computations of three years' moisture distribution profiles in the AAC wall exposed to the climatic conditions corresponding to TMY2 (Typical Meteorological Year) for Sacramento, California. The results obtained were used for calculation of the monthly average moisture content and corresponding effective thermal conductivity for the wall.

The calculation model of the AAC wall for the DOE 2.1E computer code was obtained using experimental-numerical methodology developed at ORNL (Kosny at al. 1998). This model was used to simulate a single-family residential house and commercial building located in Sacramento, California. To compare the annual energy demands of buildings constructed using AAC units and other popular North American technologies, the whole building simulations were done for the same two buildings, with the same wall thermal resistance, but constructed using steel-framed and wood-framed walls. Different air-leakage rates were considered for each type of wall material using the Sherman-Grimsrud Infiltration Method (Sherman & Grimsrud 1980).

Thermal Conductivity of Moist Lightweight Concretes

Thermal conductivity of building materials is usually tested by use of a plate apparatus based on the steady-state method. Such tests are usually done according to the ASTM C-518 procedure (ASTM 1998). When moist materials are being tested in a plate apparatus, a thermodiffusion phenomenon occurs, causing moisture migration and related latent heat transfer. We believe this is a source of considerable measurement errors.

To evaluate these possible errors and better understand the physical phenomena during steady-state tests, a computer simulation of the hygro-thermal phenomena in moist materials was performed. It is based on the mathematical model of coupled heat and mass transfer in building materials, HMTRA (Gawin & Schrefler 1996), a sophisticated, state-of-the-art mathematical model taking into account all important energy and mass transport phenomena, including phase changes (evaporation – condensation) and material deformations. Some main features of the model and information about its numerical solution are briefly summarized.

Model of Coupled Heat and Mass Transfer in Building Materials

In the HAMTRA model, building materials are treated as multiphase media, where solid skeleton voids are filled partly with liquid water (capillary and adsorbed water) and partly with a gas phase (ideal mixture of dry air and water vapor). The full model consists of the following balance equations:

- mass of solid skeleton,
- mass of dry air - considering both diffusional (flow by Fick's law) and advectional (flow by Darcy's law) molecular transport mechanisms,
- mass of the water species, both in liquid and gaseous state, taking into account phase changes, i.e., evaporation - condensation, and adsorption – desorption, as well as diffusional and advectional transport mechanisms for gas molecules,
- enthalpy of the whole medium, with latent heat of phase changes, as well as both conduction and convection energy transport considered,

- linear momentum (mechanical equilibrium) of the multiphase system, taking into account elastic deformation and thermal expansion.

These equations are completed by an appropriate set of constitutive and state equations, initial and boundary conditions, as well as some thermodynamic relationships. Temperature, capillary pressure and gas pressure dependence of several material parameters are included. The perameters are sorption isotherms, thermal conductivity and capacity, intrinsic and relative permeability, effective vapor diffusivity, Young's modulus, and Poisson's ratio. Dependencies are allowed for key physical quantities, like the specific latent heat of evaporation and adsorption, water and gas viscosity, and vapor diffusivity in the air. The governing equations of the model are expressed in terms of the chosen state variables, i.e., gas pressure p_g, capillary pressure p_c, temperature T and displacement vector of the solid matrix **u**. These equations are discretized in space using the finite element method and in time by means of the finite difference method (Zienkiewicz & Taylor 1989, 1991). Details about the numerical solution of the model equations can be found in Gawin & Schrefler 1996. Based on this mathematical model, the HMTRA-research computer code has been developed for the solution of non-linear and non-symmetrical systems of equations governing heat and mass transfer in deforming porous media. It allows convective and/or radiative boundary conditions using hourly climatic data, e.g., from Test Reference Year (TRY) or Typical Meteorological Year (TMY) data stes. The code has been successfully applied for solution of several theoretical and practical problems concerning hygro-thermal phenomena in building materials and soils (Gawin et al. 1995, 1996, 1999, Gawin & Schrefler 1996).

Computer Simulation of Steady-state Tests of AAC Thermal Conductivity

Hygro-thermal phenomena in AAC samples during steady-state tests of thermal conductivity have been numerically simulated by use of the HMTRA-DEF computer code. Computations have been done for two types of AAC, with apparent density of 400 and 600 kg/m^3, at various initial moisture contents, corresponding to thermodynamic equilibrium with the surrounding air at relative humidities of 40, 50, 60, 70, 80, 85, 90 and 95% RH. The influence of several factors, like sample thickness, plate temperature difference, initial moisture content and measurement time on the accuracy of the steady-state thermal conductivity test (i.e., ratio of measured and predicted, corresponding to homogenous moisture distribution, values of thermal conductivity) has been analyzed. These results allowed better understanding of physical phenomena causing the apparent increase of thermal conductivity and evaluation of error caused by moisture migration.

Two main reasons for these errors are an increase in heat flux caused by latent heat transfer (related to the "heat pipe" mechanism) and a decrease in heat flux due to a change in moisture distribution. The most important reason is the effect of the initial relative humidity (moisture content). In the range of 60-90% RH the "heat pipe" mechanism is of importance, causing an additional latent heat transport which apparently increases thermal conductivity up to about 6% for AC 400 kg/m^3 and up to 1.2% for AC 600 kg/m^3. These phenomena are strongly influenced by the inner structure of pores (density of AC), i.e. the shape of sorption isotherms. Outside this relative humidity range, error caused by moisture movement is negligible. The error caused by moisture is about five times smaller for AC 600 kg/m^3 than for 400 kg/m^3. The smaller the sample thickness the smaller the error. Also, the smaller the

temperature difference between plates of the apparatus, the smaller the observed moisture-induced error. On the basis of the computer simulation results several graphs and tables were developed yielding correction factors to evaluate the accuracy of the steady-state measurements of thermal conductivity for AACs. The effect of initial relative humidity, temperature difference and sample thickness upon accuracy of the steady-state test for AAC with density of 400 kg/m^3 at time t=6 hours is demonstrated in Figure 1. The effect of measurement time on the test accuracy and measured heat flux for the same AAC is shown in Figure 2.

It should be emphasized that the temperature of the sample surfaces (plates) is constant during the steady-state thermal conductivity tests, and hence every change in heat flux value indicates the existence of a test error. Moreover, constant heat flux is one of the criteria used in the plate apparatus to determine if steady-state has been achieved and the test can be terminated. Analyzing the results of the theoretical computations and some experimental tests, one can conclude that a steady-state method can be used for measurements of thermal conductivity for moist lightweight concrete in the hygroscopic moisture range, where the effect of gravity on moisture distribution is negligible. Heat flux changes caused by moisture movement and latent heat transfer are of the greatest importance for relative humidity in the range of 80-90%. But even in this range they are small enough to perform the steady-state test and obtain results with reasonable accuracy.

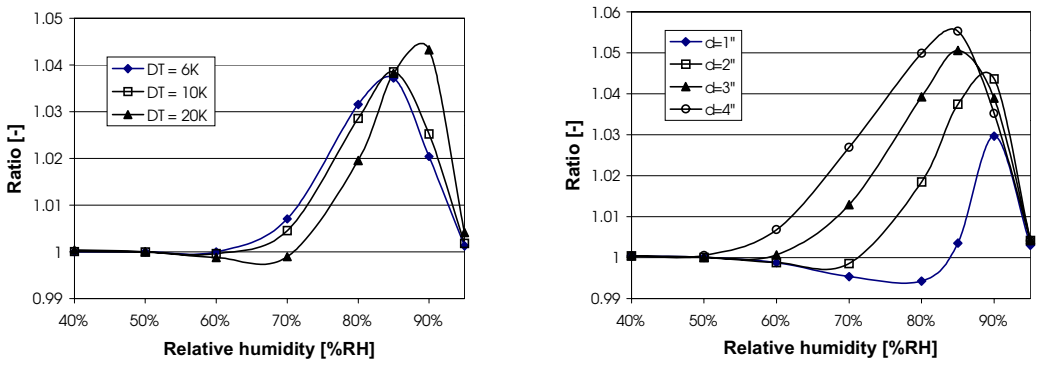

Figure 1. Ratio between measured and actual thermal conductivity vs. relative humidity of the AAC with density of 400 kg/m^3 at time t=6 hours

A) for various values of the temperature difference between plates of the apparatus

B) for various values of the sample thickness

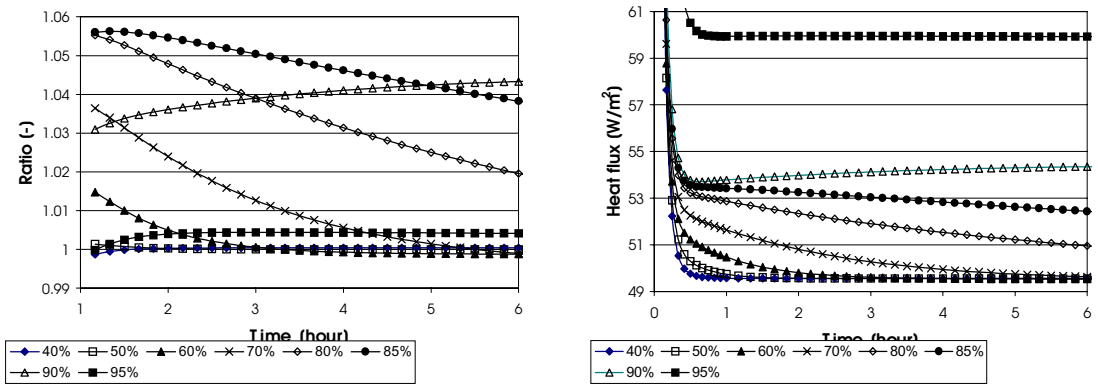

A B

Figure 2. Time history of the ratio between measured and actual thermal conductivity (A) and measured heat flux (B) for various values of the relative humidity of the AAC with density of 400 kg/m^3

Results of Steady-state Thermal Conductivity Tests for Lightweight Concretes

Thermal conductivities of three different types of AAC blocks with density of 400, 500 and 600 kg/m^3, wood concrete and EPS concrete, and various hygroscopic moisture contents, were measured in the Material Properties Laboratory following the ASTM C-518 procedure. The highest analyzed moisture contents were about 12%M, for aerated concrete and EPS-concrete samples, and about 14%M for wood- concrete.

The results of the tests are presented in Figure 3. As was expected, thermal conductivity of these moist materials is considerably higher compared to the oven dry state. The strongest influence of the mass moisture content on thermal conductivity was observed for AAC with densities of 400 kg/m^3 and 500 kg/m^3, and the lowest one for EPS-concrete. An increase of thermal conductivity in the hygroscopic moisture range is proportional to the mass moisture content. It can be approximated, with sufficient accuracy, using a linear relationship. The parameters λ_{dry} [W/(m·K)] and K [W/(m·K)] of the approximate linear relationship $\lambda = \lambda_{dry} + K \cdot u$, expressing thermal conductivity λ of the moist materials as a function of the mass moisture content, u [kg/kg], and their correlation coefficients R are presented in Table 1.

Table 1. Thermal conductivity of various types of LC as a linear function of mass moisture content

Material	λ_{dry} [W/(m·K)]	K [W/(m·K)]	R^2
AAC 400 kg/m^3	0.1125	0.0067	0.9541
AAC 500 kg/m^3	0.1407	0.0067	0.9998
AAC 600 kg/m^3	0.1597	0.0062	0.9713
Wood concrete	0.1472	0.0032	0.9847
EPS concrete	0.1089	0.0023	0.9717

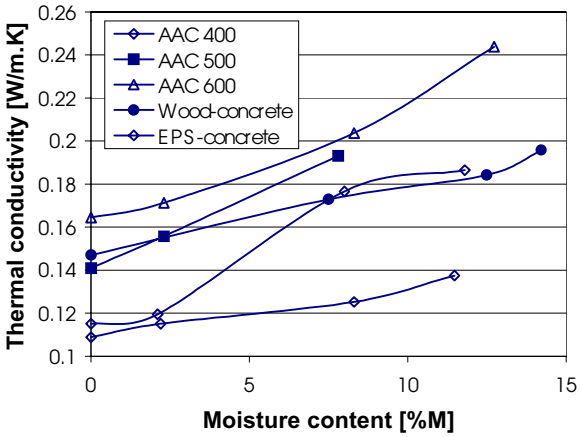

Figure 3. Results of the steady-state measurements of the thermal conductivity for various types of lightweight concrete

Some results of the tests done for the moist LC confirmed the qualitative results of the theoretical analysis. The changes in time of the measured heat fluxes were greater for moderate moisture contents than for the highest used in our tests.

Energy Performance of Buildings with AAC Walls

Results presented in the previous section indicate that thermal properties of AAC blocks are strongly influenced by their moisture content. During and after building construction, CMU walls still contain considerable moisture. In order to evaluate changes in moisture distribution and the related changes of thermal properties of the AAC walls during the first three years of building service, computer simulations have been performed. The computer code HMTRA has been used to generate moisture distribution changes for this time in the wall exposed to the climatic conditions corresponding to TMY2 for Sacramento, California.

A 19.8 cm (7.81-in.) cellular concrete wall is covered on the inside with a 0.16 cm (0.06-in.) layer of stucco and on the exterior one with 0.32 cm (0.12-in.) plaster. The material parameters assumed in the computations are shown in Table 2.

Table 2. Material parameters of the wall used in computer simulation

Material property	Units	Exterior plaster and interior stucco	Cellular concrete
Dry state apparent density, ρ_o	kg/m^3	1860	463
Porosity, Φ	-	0.16	0.78
Thermal conductivity of dry material, λ_{dry}	$W/(m \cdot K)$	0.9	0.165
Specific heat of dry material, C_{dry}	$J/(kg \cdot K)$	940	850
Intrinsic permeability, K_o	m^2	$2.0 \cdot 10^{-18}$	$2.5 \cdot 10^{-17}$
Young's modulus, E	GPa	15	1.5
Poison's ratio, ν	-	0.15	0.25

Three different cases of finish layers on the wall surfaces were analyzed:

a) both wall surfaces without vapor retarder paint,
b) interior wall surface with vapor retarder paint, exterior one without paint,
c) exterior wall surface with vapor retarder paint, interior one without paint.

For all cases, a vapor retarder paint layer thickness of 70 μm and water vapor permeance of 26 ng/(s·m^2·Pa), have been assumed (ASHRAE 1997). At the beginning of the simulation, on January 1st, the wall is assumed to be in thermodynamic equilibrium with the air, having a temperature T= 294.15 K and relative humidity φ= 95%. The RH value was assumed to take into account moisture present in the pores of the materials after construction of the wall. On the interior surface of the wall convective type boundary conditions, with air temperature T_i= 294.15 K, relative humidity φ_i=55% RH, heat surface exchange coefficient α_i= 8.0 W/ m^2·K and mass surface exchange coefficient (related to vapor density) β_i=0.008 m/s, have been assumed. On the exterior surface convective boundary conditions have been assumed, with α_e= 23.0 W/ m^2·K, β_i=0.023 m/s and temperature and relative humidity of the exterior air changing in time according to the TMY2 climatic data for Sacramento. In order to evaluate the greatest possible changes of the moisture content of the wall, and hence also its thermal properties, it has been assumed that the wall is shielded from direct contact with rain water, which could slow down their average drying rate.

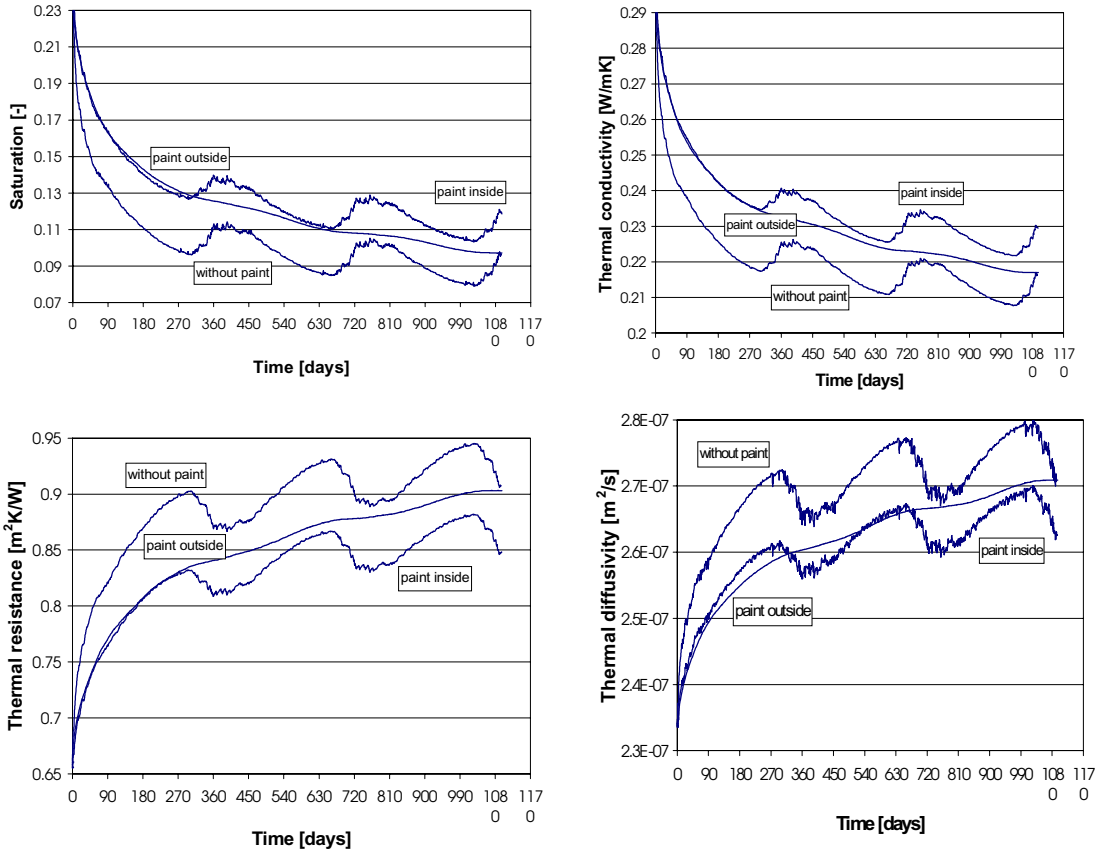

Figure 4. Time changes of the AAC-wall properties for the analyzed cases of surface finish layers, calculated for a building located in Sacramento (California)

The resulting changes of space-averaged values of pore degree of saturation with moisture (volume of liquid water / volume of pores), S, thermal conductivity, λ, thermal resistance, R_T, and thermal diffusivity, a_q, for the AAC layer are presented in Figure 4 for three cases. As is expected, distinct differences in time can be observed for all analyzed parameters. Even the fastest drying wall, without any paint on the surfaces, still contains considerable amounts of water after three years, having, on average, 10% of saturation. This caused about 30% decrease in thermal conductivity and about 40% increase in thermal resistance as shown in Figure 5. One can expect considerable changes of wall thermal performance with time, influencing the entire building energy consumption. Using the space-averaged results of computations, presented in Figure 4, the corresponding, time- and space-averaged values of moisture content, thermal conductivity, specific heat and material apparent density have been calculated for each month of the analyzed period. These averaged material properties were used in building energy performance simulations presented next.

Results of the DOE 2.1E Computations for a Residential Building

Energy performance of a single-story ranch-style house has been analyzed. The house has about 143 m^2 (1540 ft^2) of living area, 123 m^2 (1328 ft^2) of exterior wall area. The wall area includes 106 m^2 (1146 ft^2) of opaque wall , 14.3 m^2 (154 ft^2) of window area, and 2.6 m^2 (28 ft^2) of door area. The following building design characteristics and operating conditions have been used in computer modeling:

- Interior walls (made of 2×4 wood studs): 3.57 lb/ft^2 of floor area, specific heat of 0.26 Btu/lb °F;
- Furniture: 3.30 lb/ft^2 of floor area, specific heat of 0.30 Btu/lb °F, thickness of 2 in. (total equivalent floor area);
- Thermostat set point: 70°F for heating and 78°F for cooling;
- Window type: double-pane clear glass, with transmittance of 0.88 and reflectance of 0.08;
- Roof insulation with thermal resistance of R-30 h·ft^2·°F/Btu.

For calculating infiltration, the Sherman-Grimsrud Infiltration Method option in the DOE 2.1E whole building simulation model has been used. An average total leakage area of 0.0005, expressed as a fraction of the floor area, has been assumed.

Simulations have been done for Sacramento using data from the TMY2 weather data set. Space- and time- averaged material parameters of the cellular concrete wall, different for each month of the analyzed three-year period, have been used in computations to take into account, in an approximate manner, moisture distribution changes in time. Calculations have been made for the three cases of wall finish layers, separately for each month. Additionally, for comparison, two limiting cases with constant thermal properties, corresponding to initial moisture content (95% R.H.) and the dry air state, have been considered.

Results of the DOE 2.1E calculations for electrical energy and natural gas energy consumption during the first 12 months for the next two years are presented in Figure 5. Various moisture contents, resulting from different finish layers of the wall, may cause approximately 18.5% increase of monthly energy consumption in December and January as compared to the building with dry walls. With an increase in the average wall moisture content, the electrical energy consumption decreases in summer (up to 18%) and increases the gas energy for heating in winter (up to 19%).

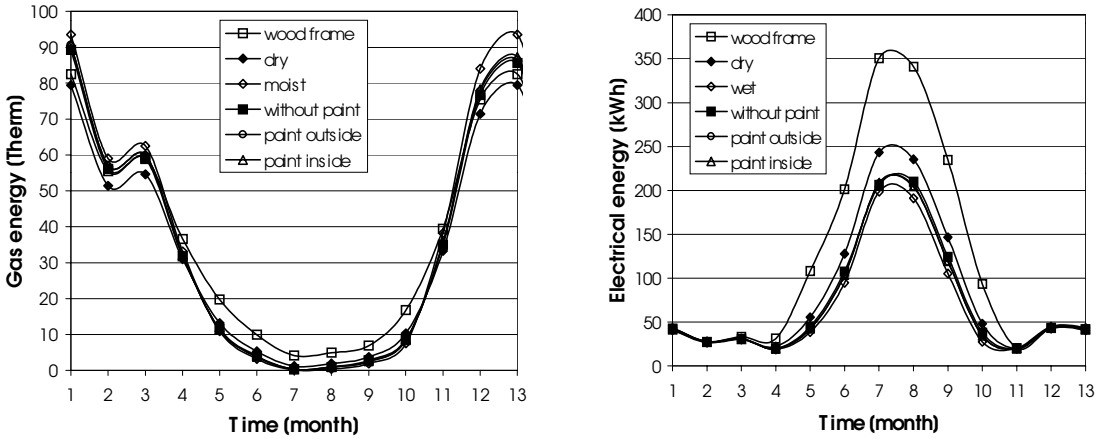

Figure 5. Comparison of Natural Gas- and Electrical Energy Consumption During the First Year, Simulated by Means of the DOE 2.1E Model for a Residential Building, with Wood-framed Walls and the Analyzed Cases of AAC Walls, Located in Sacramento (California).

Table 3. Comparison of the annual energy consumption in a residential building for various wall finish layers against the dried wall case for Sacramento (California)

Year of service time	Moist wall	Wall without paint	Wall with outside paint	Wall with inside paint	Wood frame wall
Total energy					
1	107.9%	103.9%	104.6%	105.0%	118.1%
2	107.9%	102.3%	102.6%	103.3%	118.1%
3	107.9%	102.1%	102.0%	103.1%	118.1%
Electrical energy					
1	81.1%	88.0%	86.2%	86.5%	146.9%
2	81.1%	90.0%	88.0%	88.0%	146.9%
3	81.1%	90.6%	89.0%	88.5%	146.9%
Natural gas energy					
1	110.5%	105.4%	106.5%	106.9%	115.2%
2	110.5%	103.5%	104.0%	104.9%	115.2%
3	110.5%	103.2%	103.3%	104.6%	115.2%

To better analyze the effect of the AAC-wall finish layers on the whole building energy performance during the first three years of building use, the yearly consumption of total electrical and natural gas energy are compared in Table 3 against the results obtained for the building with dry AAC walls. Additionally, results for the same building, but with wood-framed walls of the same thermal resistance as the AAC walls (without vapor retarder paint) at the end of the three year period, are shown. The energy consumption for this building is the highest of all cases, even with completely moist AAC walls. The difference it causes is most evident during summer, when electrical energy is used for air-conditioning. This is due to the lack of inherent thermal mass effect. Lack of thermal mass is also important during

winter, when its effect exceeds some additional heat losses caused by a moisture-induced decrease of the AAC-wall thermal resistance.

Results of the DOE 2.1E Computations for a Commercial Building

Energy performance of a one-story 1092 m^2 (11,760 ft^2) retail store has been analyzed. The building has 648 m^2 (6,976 ft^2) of exterior wall area and 106 m^2 (1,144 ft^2) of window area. The following building design characteristics and operating conditions have been used in computer modeling:

- Thermostat set point: 70°F for heating and 76°F for cooling;
- Window type: double-pane clear glass, with transmittance of 0.88 and reflectance of 0.08;
- Roof insulation with thermal resistance of R-30 $h \cdot ft^2 \cdot °F/Btu$ (5.28 m^2 K/W).

Climatic data from the TMY2 data set for Sacramento have been used. Calculations have been done for the same thee wall finish layers as in the previous section, separately for each month, using space- and time- averaged material parameters of AAC. Additionally, for comparison, two limiting cases with constant thermal properties, corresponding to initial moisture content (95% R.H.) and the air dry state, have been considered.

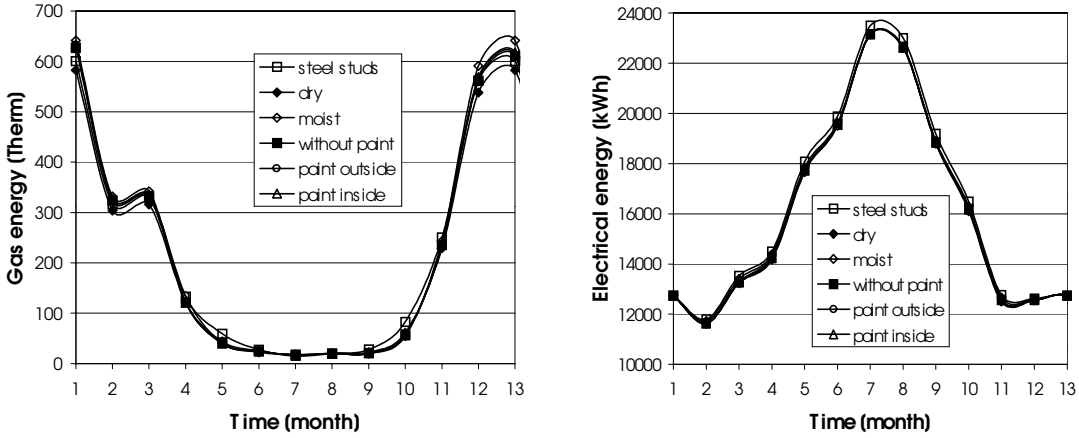

Figure 6. Comparison of the Natural Gas- and Electrical Energy Consumption During the First Year, Simulated by Means of the DOE 2.1E Model for a Commercial Building, with Steel-framed Walls and the Analyzed Cases of AAC Walls, Located in Sacramento (California)

Results of the DOE 2.1E calculations, yielding electrical energy and natural gas energy consumption during the first twelve months are presented in Figure 6. The changes with time during the next two years are similar. The yearly consumption of total electrical and natural gas energy are compared in Table 4 to the results obtained for the building with the dry AAC-walls. Results are shown for the same building, but with steel-framed walls of the same thermal resistance as the AAC-walls (without vapor retarder paint). The energy consumption for steel-framed case is the highest of all the cases for the retail mall building with AAC-walls, except the moist AAC wall case. For commercial buildings wall heat losses are of less importance for the whole building energy performance than in residential buildings. But even for this type of building, inherent thermal mass effects can reduce the whole building energy consumption.

Table 4. Comparison of commercial building energy consumption for various wall finish layers against the dry wall case for Sacramento (California)

Year of building exploitation	Moist wall	Wall Without paint	Wall with outside paint	Wall with inside paint	Steel stud wall
Total energy					
1	101.30%	100.79%	101.10%	100.95%	102.38%
2	101.30%	100.50%	100.55%	100.68%	102.38%
3	101.30%	100.46%	100.47%	100.64%	102.38%
Electrical energy					
1	99.29%	99.57%	99.55%	99.49%	101.04%
2	99.29%	99.64%	99.58%	99.56%	101.04%
3	99.29%	99.66%	99.62%	99.58%	101.04%
Natural gas energy					
1	107.19%	104.36%	105.62%	105.23%	106.30%
2	107.19%	103.04%	103.42%	103.99%	106.30%
3	107.19%	102.81%	102.96%	103.73%	106.30%

Conclusions

Computer simulations have shown that a steady-state method to measure thermal conductivity is applicable for moist lightweight concretes in the hygroscopic moisture content range, giving acceptable measurement accuracy. According to the simulations, additional error caused by moisture movement and latent heat transfer does not exceed 6% for the AAC with density of 400 kg/m^3, where one can expect the greater effect of these phenomena because of the high porosity value and open internal structure of the material.

The thermal conductivity of five different types of LC, at various hygroscopic moisture contents, was measured following the ASTM C-518 (steady-state) procedure. Linear relationships adequately expressed thermal conductivity of the moist materials as a function of moisture content. Thermal conductivity of LCs is strongly dependent on moisture content, especially for AAC.

Changes of moisture distribution in the AAC wall were computed for California climatic conditions using the HMTRA computer model of coupled heat and moisture transfer in building materials. Using these results, monthly average moisture contents were calculated for evaluation of effective thermal properties of the LC wall for three years after building construction.

These data used in DOE 2.1E computer simulations showed a moisture-caused decrease in thermal resistance. However the annual energy demands of the building with LC walls were lower in comparison to other technologies, both for residential and commercial buildings, due to the inherent thermal mass effect. This effect was most evident for the residential building, especially during summer.

LCs are building materials whose application to construction of residential and commercial buildings can bring considerable cooling and heating energy savings compared to other technologies, when walls with the same thermal resistance are used. The decrease of

LC-wall thermal resistance due to the higher moisture content may partly reduce this advantage.

Acknowledgement

Dariusz Gawin was supported in part for this research by an appointment to the Oak Ridge National Laboratory Postdoctoral Research Associates Program administrated jointly by the Oak Ridge Institute for Science and Education and Oak Ridge National Laboratory.

References

ASTM. 1998. C 518-98. *Standard Test Method for Steady-State Thermal Transmission Properties by Means of the Heat Flow Meter Apparatus*, West Conshohocken, Pa.: American Society for Testing and Materials.

ASHRAE. 1997. *Fundamentals*, Atlanta, Ga.: American Society of Heating, Refrigerating and Air-Conditioning Engineers.

Gawin D., P. Baggio., & B.A. Schrefler 1995. "Coupled heat, water and gas flow in deformable porous media," *Int. J. Num. Meth. in Fluids, 20: 969-987* .

Gawin D. & B.A. Schrefler 1996. "Thermo- hydro- mechanical analysis of partially saturated porous materials," *Engineering Computations, 13, No.7: 113-143*

Gawin D., P. Baggio., & B.A. Schrefler 1996. "Modelling heat and moisture transfer in deformable porous building materials," *Arch. of Civil Engineering*, *42: 325-349*

Gawin D., C.E. Majorana, & B.A. Schrefler 1999. "Numerical analysis of hygro-thermic behaviour and damage of concrete at high temperature," *Mechanics of Cohesive-Frictional Materials*, *4: 37-74*

Kosny J. 1994, "Wooden Concrete – High Thermal Efficiency Using waste Wood" In *proceedings of ACEEE Summer Study Conference.* August. Pacific Grove, California

Kosny J, E. Kossecka, A. O. Desjarlais, J. Christian 1998, "Dynamic Thermal Performance of Concrete and Masonry Walls " – In *proceedings of DOE, ASHRAE, ORNL Conference - Thermal Envelopes VII*. December. Clear Water, Florida.

Sherman M.H. & D.T. Grimsrud, 1980, *"Measurement of Infiltration Using Fan Pressurization and Weather Data", LBL-10852, Berkeley Calif: Lawrence Berkeley National Laboratory.*

Zienkiewicz O.C. & R.L. Taylor 1989. *The Finite Element Method, 1, (4th ed.) London: Mc Graw Hill.*

Zienkiewicz O.C. & R.L. Taylor 1991. *The Finite Element Method, 2, (4th ed.) London: Mc Graw Hill.*